Receptor activator of nuclear factor (NF)–κB ligand (RANKL) increases vascular permeability: impaired permeability and angiogenesis in eNOS-deficient mice

Jeong-Ki Min,[1] Young-Lai Cho,[2] Jae-Hoon Choi,[3] Yonghak Kim,[1] Jeong Hun Kim,[4,5] Young Suk Yu,[4,5] Jaerang Rho,[6] Naoki Mochizuki,[7] Young-Myeong Kim,[2] Goo Taeg Oh,[3] and Young-Guen Kwon[1]

[1]Department of Biochemistry, College of Sciences, Yonsei University, Seoul, Republic of Korea; [2]Department of Molecular and Cellular Biochemistry, School of Medicine, Kangwon National University, Chunchon, Kangwon-Do, Republic of Korea; [4]Department of Ophthalmology, Seoul National University College of Medicine, Seoul National University Hospital, Seoul, Republic of Korea; [5]Seoul Artificial Eye Center, Clinical Research Institute, Seoul National University Hospital, Republic of Korea; [7]Department of Structural Analysis, National Cardiovascular Center Research Institute, Osaka, Japan; [6]Department of Microbiology, College of Natural Sciences, Chungnam National University, Daejeon, Republic of Korea; [3]Division of Molecular Life Science, Ewha Womans University, Seoul, Republic of Korea

Receptor activator of nuclear factor (NF)–κB ligand (RANKL) is emerging as an important regulator of vascular pathophysiology. Here, we demonstrate a novel role of RANKL as a vascular permeability factor and a critical role of endothelial nitric oxide synthase (eNOS) in RANKL-induced endothelial function. RANKL increased the vascular permeability and leukocyte infiltration in vivo and caused the breakdown of the blood-retinal barrier in wild-type mice but not in eNOS-deficient mice. In vitro, it increased endothelial permeability and reduced VE-cadherin–facilitated endothelial cell-cell junctions in a NO-dependent manner. RANKL also led to the activation of Akt and eNOS and to NO production in endothelial cells (ECs). These effects were suppressed by the inhibition of TRAF6, phosphoinositide 3′-kinase (PI3K), Akt, or NOS by genetic or pharmacologic means. Inhibition of the TRAF6-mediated NO pathway reduced EC migration and capillary-like tube formation in response to RANKL. Moreover, the effects of RANKL on ECs sprouting from the aorta, and neovessel formation in both the mouse Matrigel plug assay and corneal micropocket assay, were impaired in eNOS-deficient mice. These results demonstrate that RANKL promotes vascular permeability and angiogenesis by stimulating eNOS by a TRAF6-PI3K-Akt–dependent mechanism. These properties may be relevant to the pathogenesis of angiogenesis-dependent and inflammatory vascular diseases. (Blood. 2007;109:1495-1502)

Introduction

Angiogenesis, the formation of new blood vessels from a preexisting vascular bed, is a pivotal process not only in embryonic development but also in the progression of a variety of pathologic conditions.[1] A large number of molecules, which are composed of growth factors, cytokines, and lipid metabolites, are shown to be involved in pathophysiologic neovascularization by stimulating endothelial cells (ECs) directly or indirectly.[2] Some of these factors, including VEGF, often possess their abilities to increase vascular permeability and thus contribute to deteriorating tissue damage.

Receptor activator of nuclear factor (NF)–κB ligand (RANKL), also known as ODF, TRANCE, and OPGL, has well-understood roles in the skeletal and immune systems in which it induces osteoclast differentiation from hematopoietic precursors and regulates the function and survival of dendritic cells.[3] Recently, interest has grown in its physiologic and pathologic relevance to vascular biology.[4] Mounting evidence suggests that RANKL and its decoy receptor, osteoprotegrin (OPG), participate in multiple aspects of vascular calcification; for example, mice lacking OPG suffer late medial calcification of the renal and aortic arteries in addition to early onset osteoporosis.[5-7] Moreover, a role for the OPG/RANKL/RANK axis in atherogenesis and plaque destabilization has been recently reported.[8] OPG inactivation accelerates advanced atherosclerotic lesion progression and calcification in older ApoE$^{-/-}$ mice.[9] TRANCE is strongly expressed in vascular cells in vitro, as well as in vivo. OPG and it are induced by inflammatory cytokines in human ECs, although with different temporal profiles.[10] In vivo, RANKL is present in the small blood vessels of the skin and in arterial smooth muscle cells,[11] and it appears to be up-regulated in atherosclerotic lesions, calcified vessels, and valves.[4,6,9] Moreover, the RANKL receptor, RANK, is also expressed in ECs of the rat coronary artery and developing blood vessels of the rat embryo in vivo, as well as in freshly isolated human umbilical vein ECs (HUVECs).[12] In agreement with these patterns of expression, RANKL stimulates the survival of cultured ECs and their production of inflammatory cell adhesion molecules; it also promotes in vitro angiogenesis by the ECs and elicits neoangiogenesis in animal models.[13] Moreover, VEGF increases RANK mRNA and protein in ECs, augmenting their angiogenic response to RANKL.[12] Therefore, the RANKL/RANK/OPG system is believed to be an important link between the vascular, skeletal, and immune systems.

Endothelium-derived nitric oxide (NO), originally identified as endothelium-derived relaxing factor, promotes angiogenesis and plays an important role in vascular remodeling and the maintenance of vascular integrity.[14,15] In ECs, NO is a product of the

Submitted June 14, 2006; accepted September 29, 2006. Prepublished online as *Blood* First Edition Paper, October 12, 2006; DOI 10.1182/blood-2006-06-029298.

The online version of this article contains a data supplement.

An Inside *Blood* analysis of this article appears at the front of this issue.

The publication costs of this article were defrayed in part by page charge payment. Therefore, and solely to indicate this fact, this article is hereby marked "advertisement" in accordance with 18 USC section 1734.

conversion of L-arginine to citrulline by endothelial NO synthase (eNOS). eNOS produces low levels of NO constitutively but can be transiently stimulated to produce high levels by various hormones and environmental stimuli such as vascular endothelial growth factor (VEGF), angiopoietin-1, shear stress, and hypoxia.[16,17] Moreover, eNOS knockout (KO) mice exhibit impaired postnatal angiogenesis in response to tissue ischemia.[15,16] Although the mechanisms by which it promotes angiogenesis is not fully elucidated, NO has emerged as an important modulator of endothelial activation underlying physiologic and pathologic angiogenesis and inflammation.

The increased expression of RANKL in the injured blood vessels suggests the involvement of RANKL in vascular pathophysiology. However, little information is available for its vascular function and underlying signaling mechanisms in ECs. In the present study, our data demonstrate that RANKL has a significant effect on vascular permeability, which is governed by interendothelial junctions between adjacent cells. We further present genetic and pharmacologic evidence that endothelium-derived NO plays a critical role in promoting the vascular permeability and angiogenesis induced by RANKL.

Materials and methods

Cell culture and reagents

HUVECs were isolated from human umbilical cord veins by collagenase treatment, as described previously,[18] and were used in passages 2 to 7. They were grown in M199 medium (Invitrogen, Carlsbad, CA) supplemented with 20% fetal bovine serum (FBS). Soluble RANKL (hCD8-conjugated form) was purified from insect cells as described previously.[15]

Endothelial-cell migration assay

Chemotactic motility of HUVECs was assayed as described previously.[19] Briefly, the lower surface of the filter was coated with 10 μg gelatin. Fresh M199 medium (1% FBS) containing RANKL was placed in the lower wells. The cells were trypsinized and suspended at a final concentration of 1×10^6 cells/mL in M199 containing 1% FBS. One hundred microliters of the cell suspension was loaded into each of the upper wells, and the chamber was incubated at 37°C for 4 hours. The cells were fixed and stained with hematoxylin and eosin. Nonmigrating cells on the upper surface of the filter were removed by wiping with a cotton swab, and chemotaxis was quantified with an optical microscope (× 200) by counting cells that had migrated to the lower side of the filter. Ten fields were counted for each assay.

Tube formation assay

Tube formation was assayed as previously described.[19] Briefly, 250 μL growth factor-reduced Matrigel (10 mg protein/mL) was pipetted into a 16-mm diameter tissue culture well and polymerized for 30 minutes at 37°C. HUVECs incubated in M199 containing 1% FBS for 6 hours were harvested after trypsin treatment, resuspended in M199, plated onto the layer of Matrigel at a density of 1.8×10^5 cells/well, and RANKL was added. After 20 hours, the cultures were photographed (× 200). The area covered by the tube network was measured using an optical imaging technique in which pictures of the tubes were scanned in Adobe Photoshop (San Diego, CA) and quantified with Image-Pro Plus (Media Cybernetics, Silver Spring, MD).

Retroviral vectors and generation of stable transfectants

cDNA sequences encoding hemagglutinin (HA)–tagged dominant-negative TRAF2 (DN-T2) and Flag-tagged dominant-negative TRAF6 (DN-T6) were subcloned into pMSCVpuro vector (Clontech, Palo Alto, CA) and introduced into HEK293T cells (packaging cell line) with 1 μg pVSV-G vector (Clontech) using LipofectAMINE Plus reagent according to the manufacturer's instructions. The next day, the virus in the supernatants of these cells was added to HUVECs along with 5 μg/mL polybrene. After 24 hours of incubation, the medium was removed and replaced with fresh medium containing 3 μg/mL puromycin. Puromycin-resistant clones were selected by incubating for 1 week in the presence of 3 μg/mL puromycin. Protein expression was confirmed by Western blotting.

[^{3}H] Sucrose permeability assay

HUVECs were plated onto a Transwell filter (Corning Costar, Cambridge MA). After reaching confluence, HUVECs were incubated with M199 containing 1% FBS for 3 hours and treated with various concentrations of RANKL (0.5, 1, and 5 μg/mL) or 20 ng/mL VEGF for 1 hour. Fifty microliters (0.8 μCi [0.0296 MBq]/mL) of [^{3}H]sucrose (1 μCi [0.037 MBq]/μL; Amersham Pharmacia, Bucks, United Kingdom) was added to the upper compartment. The amount of radioactivity that diffused into the lower compartment was determined after 30 minutes by liquid scintillation counter (Perkin Elmer/Wallac, Gaithersburg, MD).

Miles vascular permeability assay

Miles assay was performed as described previously.[20] Evans blue dye (100 μL of a 1% solution in 0.9% NaCl) was injected into the tail vein of C57BL/6 wild-type (WT) and eNOS KO mice (n = 7 per group). After 10 minutes, RANKL (10 μg in 10 μL PBS) was injected intradermally into the shaved back skin of mice. After 20 minutes, the animals were killed, and an area of skin that included the blue spot resulting from leakage of the dye was removed. Evans blue dye was extracted from the skin by incubation with formamide for 4 days at room temperature, and the absorbance of the extracted dye was measured at 620 nm with a spectrophotometer.

Perfusion of FITC-dextran

C57BL/6 WT and eNOS KO mice (8-10 weeks old, n = 7 per group) were examined for vascular leakage after injection of RANKL. RANKL (10 μg) or PBS was injected slowly into the vitreous cavity. After 24 hours, the mice were deeply anaesthetized using ketamine/xylazine and received an intravenous injection of 10 mg FITC-dextran (MW = 20 000 D; Sigma, St Louis, MO). After 30 minutes, the eyes were enucleated and immediately fixed in 4% paraformaldehyde. The retinas were dissected out, cut in a Maltese cross configuration, flat-mounted on glass slides, and viewed with an Axioplan 2 fluorescence microscope equipped with a Zeiss Plan-Neofluar 20×/0.50 NA objective lens (Zeiss, Gottingen, Germany). The vascular permeability was quantified by counting sites with extravasation of fluorescence at postcapillary vessel.

VE-cadherin translocation assay

HUVECs plated in 6-well plates were serum starved in medium 199 containing 1% FBS for 6 hours. They were then stimulated with 5 μg/mL RANKL for 1 hour and fractionated in cytoskeleton-stabilizing buffer (10 mM HEPES [pH 7.4], 250 mM sucrose, 150 mM KCl, 1 mM EGTA, 3 mM $MgCl_2$, 1 × protease inhibitor cocktail [Roche Diagnostics, Mannheim, Germany], 1 mM Na_3VO_4, 0.5% Triton X-100) by centrifugation at 15 000*g* for 15 minutes. The proteins in the Triton X-100–insoluble and insoluble fractions were analyzed by Western blotting.

Measurement of nitrite plus nitrate

Production of nitrite plus nitrate (NOx) was measured by the ozone-chemiluminescence method. Culture media from HUVECs were collected and assayed for NOx using a chemiluminescent NO analyzer (Antek Instruments, Houston, TX),[21] and quantified with sodium nitrate as standard.

eNOS activity assay

HUVECs were detached with PBS/EDTA (1 mM) and homogenized in 10 mM Tris-HCl pH 7.4. [^{3}H]-L-arginine to [^{3}H]-L-citrulline conversion was measured with 1 mM $CaCl_2$ with or without L-NAME (1 mM) using a NOS assay kit (Calbiochem, San Diego, CA).

In vivo Matrigel plug assay

Matrigel plug assays were performed as previously described.[22] Briefly, WT and eNOS KO mice (n = 7 per group) were injected subcutaneously with 0.6 mL Matrigel containing RANKL and 15 U heparin. The injected Matrigel rapidly formed a single, solid gel plug. After 7 days, the skin of the mouse could be easily pulled back to expose the Matrigel plug, which remained intact. Hemoglobin was measured by the Drabkin method with Drabkin reagent kit 525 (Sigma) to quantify blood vessel formation. The concentration of hemoglobin was calculated from a known amount of hemoglobin assayed in parallel. To identify infiltrating endothelial cells, immunohistochemistry was performed with anti-CD31 antibody.

Aortic ring assay

Aortas were harvested from 6-week-old male Sprague Dawley rats, 6- to 8-week-old C57BL/6 WT, and eNOS KO mice. Plates (48-well) were coated with 100 μL Matrigel, and, after it had gelled, the rings were placed in the wells and sealed in place with an overlay of 40 μL Matrigel. RANKL and inhibitors were added to the wells in a final volume of 200 μL human endothelial serum-free medium (Invitrogen). On day 6, cells were fixed and stained with Diff-Quick. The assays were scored, double blind, from 0 (least positive) to 5 (most positive). Each data point was assayed in sextuplet.

Mouse corneal angiogenesis assay

Eight-week-old male C57BL/6 WT and eNOS KO mice (n = 7 per group) were used. After systemic and local eye anesthesia, a central, intrastromal linear keratotomy approximately 0.6 mm in length was performed with a surgical blade, and a micropocket was dissected toward the temporal limbus with a modified von Graefe knife. A sucrose aluminum sulfate pellet coated with Hydron polymer containing control buffer or RANKL (10 μg/pellet) was positioned 0.6 to 0.8 mm from the corneal limbus. On postoperative day 6, we measured the arc of the corneal circumference occupied by angiogenesis (circumferential angiogenesis, in degrees) and vessel lengths and numbers.

Leukocyte infiltration

Eight-week-old male C57BL/6 WT and eNOS KO mice were anesthetized and received a topical application of RANKL (3 μg/mL) or PBS. Twenty-four hours after RANKL application, the retroorbital venous sinus of each animal was injected intravenously with 200 μL biotinylated *Lycopersicon esculentum* lectin (1 mg/mL; Vector Laboratories, Burlingame, CA), which binds to *N*-acetyl-D-glucosamine residues on the luminal surface of vascular endothelial cells.[23] To perfuse the mice, the chest cavity was opened, and the atria were cut to allow outflow of blood and perfusate. Mice were perfused with a fixative (1% paraformaldehyde, 0.5% glutaraldehyde in PBS) via the left ventricle. The ears were removed, and the vascular architecture was analyzed in whole mounts of mouse ears, using a ZEISS AxioSkop2 microscope equipped with a Plan-Apochromat 40×/0.75 NA oil-immersion objective lens. Images of blood vessels and infiltrated leukocytes were captured using a ZEISS AxioCam camera with AxioVision 3.0 software.

Statistical analysis

Data are presented as mean ± SD or ± SE. Statistical comparisons between groups were performed using one-way ANOVA followed by Student *t* test.

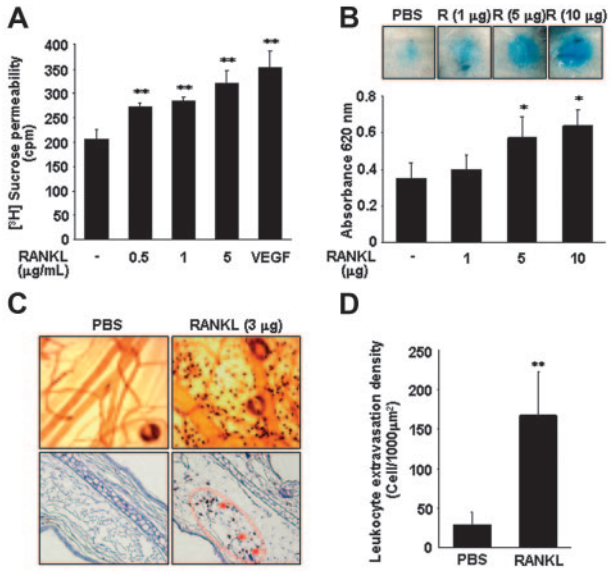

Figure 1. RANKL induces vascular hyperpermeability and leukocyte extravasation. (A) An in vitro [^{3}H]sucrose permeability assay was performed as described in "Materials and methods." Three independent experiments were performed in duplicate. Data are means ± SEs; $^{**}P < .01$ versus untreated control. (B) In vivo Miles vascular permeability assay. Various concentrations of RANKL (R) or PBS were injected intradermally into the skin of C57BL/6 mice (n = 7 per group) after intravenous injection of Evans blue. Representative picture (top) and quantity (bottom) of extravasated Evans blue in the mouse skin. Data are means ± SDs; $^{*}P < .05$ versus PBS. (C) Leukocyte extravasation. Twenty-four hours after RANKL (3 μg) application as described in "Materials and methods," mice (n = 5 per group) were perfused with the lectin *L esculentum* to visualize extravasated leukocytes (top). This experiment was performed twice. Leukocytes in the ear sections were immunostained with anti-CD11a antibody (bottom). Arrows indicate extravasated CD11a$^+$ leukocytes. (D) Quantitative analysis of extravasated leukocytes. Data are means ± SDs; $^{**}P < .01$ versus PBS.

Results

RANKL induces vascular hyperpermeability and leukocyte extravasation

Human CD8-conjugated soluble RANKL increased [^{3}H] sucrose diffusion through the pores of Transwell membranes in HUVEC monolayer culture in a dose-dependent manner (Figure 1A). The near maximal activity at 5 μg/mL was comparable to that achieved with 20 ng/mL VEGF. To test whether RANKL induces vascular hyperpermeability in vivo, a modified Miles vascular permeability assay was performed using intravenous injection of Evans blue followed by intradermal injection of RANKL. RANKL strongly induced vascular hyperpermeability in the mouse skin, as shown by the increased leakage of Evans blue (Figure 1B). Spectrophotometric measurements of the extravasated Evans blue revealed that the increase was dose dependent (Figure 1B). We further investigated the effect of RANKL on leukocyte extravasation in vivo. The mice received an ear inoculation of vehicle or RANKL for 24 hours, and then leukocyte infiltration was monitored by in vivo perfusions with the lectin *L esculentum*. RANKL-treated mice showed a dramatic increase in leukocyte extravasation, as compared with vehicle-treated mice (Figure 1C). The identity of extravasated leukocytes was confirmed by CD11a staining in the ear section (Figure 1D).

Impairment of RANKL-induced vascular hyperpermeability in eNOS-deficient mice

The role of endothelial NO in RANKL-induced vascular permeability was evaluated. The NO synthase inhibitor NMA

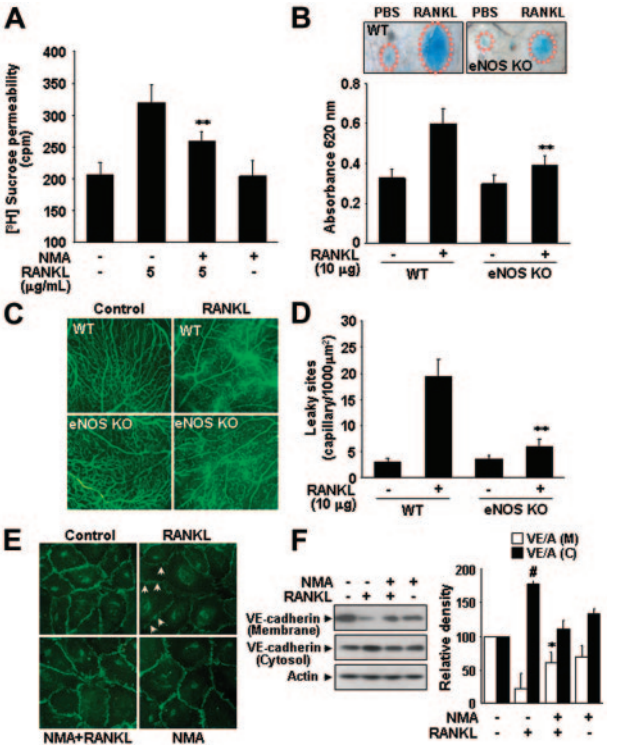

Figure 2. Impairment of RANKL-induced vascular hyperpermeability in eNOS-deficient mice. (A) HUVECs were preincubated for 30 minutes with or without NMA (1 mM) and stimulated with 5 μg/mL RANKL for 1 hour. A [3H]sucrose permeability assay was then performed. Three independent experiments were performed in duplicate. Data are means ± SEs; $^{**}P < .01$ versus RANKL alone. (B) An in vivo Miles vascular permeability assay was performed in WT and eNOS KO mice (n = 7 per group) as described in Figure 1. Data are means ± SDs; $^{**}P < .01$ versus RANKL in eNOS KO. (C) Representative fluorescence images of retinal vessels. RANKL (10 μg) or PBS was injected into the vitreous cavity of WT and eNOS KO mice (n = 7 per group). After 24 hours, the mice received an intravenous injection of 10 mg FITC-dextran (MW = 20 000 D), and their retinas were flat-mounted. (D) The vascular permeability was quantified by counting sites with extravasation of fluorescence at postcapillary vessel. Data are means ± SDs; $^{**}P < .01$ versus RANKL in eNOS KO. (E-F) HUVECs were preincubated for 30 minutes with or without NMA (1 mM) and stimulated with 5 μg/mL RANKL for 1 hour. (E) An immunofluorescence analysis of VE-cadherin. Arrows indicate disruption of VE-cadherin. (F) Translocation of VE-cadherin was assessed as described in "Materials and methods." The Triton X-100–insoluble and soluble fractions were subjected to SDS–polyacrylamide gel electrophoresis followed by Western blot analysis with anti–VE-cadherin. Blots are representative of 3 independent experiments. Densitometric analyses are presented as the relative ratio of VE-cadherin to actin. VE indicates VE-cadherin; A, actin; M, membrane; C, cytosol. Data are means ± SDs; $^{*}P < .05$ versus RANKL alone; $\#P < .05$ versus untreated control.

significantly abrogated RANKL-induced endothelial permeability in vitro (Figure 2A). Consistently, vascular hyperpermeability of the mouse skin by RANKL was substantially impaired in the eNOS KO mice compared with WT mice (Figure 2B). We further investigated the role of eNOS in retinal vascular permeability that is caused by breakdown of tight junctions between the retinal vascular endothelial cells. As shown in Figure 2C-D, injection of RANKL into the vitreous cavity of WT mice induced marked retinal vascular leakage as evidenced by the widespread, diffuse fluorescence. By contrast, the retinal vessels of the eNOS KO mice remained clearly delineated, with little or no leakage. Furthermore, the effect of RANKL on leukocyte extravasation in vivo was significantly abrogated in eNOS KO mice compared with WT mice (Figure S1A-B, available on the *Blood* website; see the Supplemental Figures link at the top of the online article).

Vascular endothelial permeability is maintained by the endothelial junction proteins, VE-cadherin, and occludin.[24] The effect of RANKL on adherens junction (AJ) formation was examined by immunostaining with anti–VE-cadherin. In confluent ECs, VE-cadherin is located at cell-cell contacts. When HUVECs were treated with RANKL, the level of VE-cadherin at cell-cell junctions markedly decreased, and pretreatment with NMA blocked this effect (Figure 2E). Normally, VE-cadherin that is anchored to the actin cytoskeleton is detected in the detergent-insoluble fractions of cell lysates.[25] There was a decrease in VE-cadherin in the Triton X-100–insoluble fraction and a concomitant increase in the Triton X-100–soluble fraction after stimulation with RANKL. This effect was reversed by NMA (Figure 2F). Taken together, these results demonstrate that RANKL induces vascular hyperpermeability in an NO-dependent manner by promoting the breakdown of endothelial AJs.

RANKL induces eNOS activation and NO production via a TRAF6/PI3K/Akt signaling pathway

To confirm whether RANKL stimulates NO production in endothelial cells, quiescent HUVECs were stimulated with RANKL and assayed for NO production and eNOS activity. RANKL increased NO production and eNOS activity (Figure 3A-B), without affecting the expression of eNOS protein (Figure 3C). The eNOS activity was evidently increased at 0.5 hours after RANKL treatment and sustained up to 24 hours (Figure 3B). eNOS is an isoform of NO synthase that is constitutively expressed in HUVECs and activated

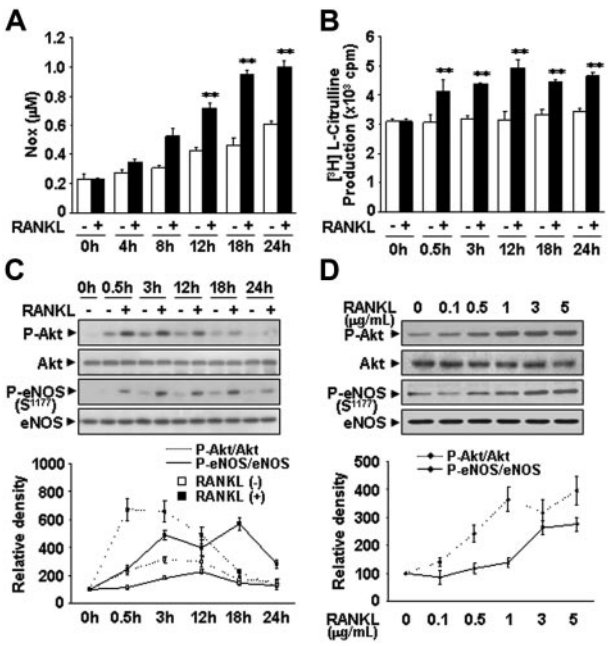

Figure 3. RANKL induces eNOS activation and NO production in endothelial cells. (A-D) HUVECs were stimulated with 5 μg/mL RANKL for the indicated times (A-C) and with various concentrations of RANKL for 30 minutes (D). (A) Levels of NOx was determined in the culture medium by using a chemiluminescent NO analyzer. (B) The eNOS enzymatic activity was measured by the production of [3H]-L-citrulline from [3H]-L-arginine. Three independent experiments were performed in duplicate. Data are means ± SEs. Statistical analysis of the results was carried out using ANOVA. $^{**}P < .01$ versus untreated control in 0 hour and each time point. (C-D) The levels of eNOS protein and phosphorylation of Akt and eNOS by RANKL were determined by Western blotting (top). Blots are representative of 3 independent experiments. Densitometric analyses are presented as the relative ratio of P-Akt to Akt and P-eNOS to eNOS. The relative ratio in untreated control is arbitrarily presented as 100 (bottom).

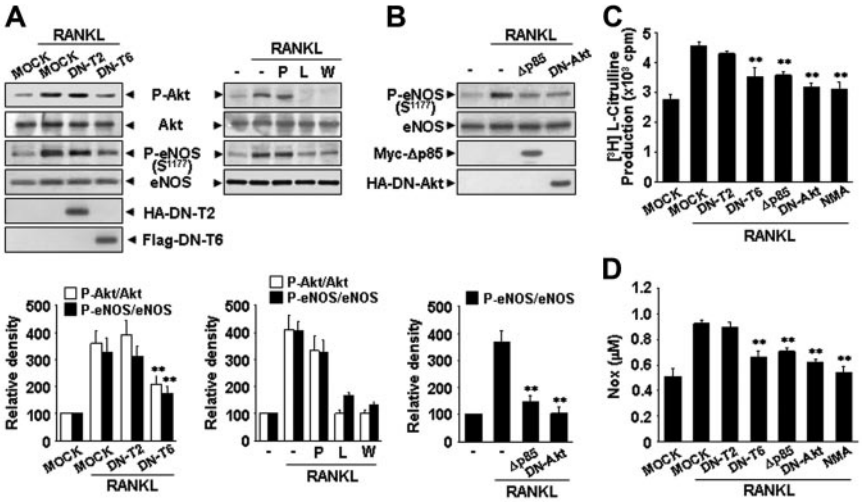

Figure 4. RANKL induces eNOS activation and NO production via a TRAF6/PI3K/Akt signaling pathway. (A) HUVECs were stably transfected with a HA-tagged DN-T2 and a Flag-tagged DN-T6 using retroviral system (left). HUVECs were preincubated for 30 minutes with or without 5 μM PP1, 100 nM Wortmannin, or 1 mM NMA prior to stimulation with RANKL (5 μg/mL) for 20 minutes (right). (B) HUVECs were transiently transfected with a HA-tagged DN-Akt or a Myc-tagged Δp85. (A-B) The levels of eNOS protein and the phosphorylation of Akt and eNOS by RANKL were determined by Western blotting (top). Blots are representative of 3 independent experiments. Densitometric analyses are presented as the relative ratio of P-Akt to Akt and P-eNOS to eNOS (bottom). (C-D) eNOS activity and NO production were measured as described in Figure 3A-B. Three independent experiments were performed in duplicate. Data are means ± SDs; $^{**}P < .01$ versus RANKL alone.

by Akt-mediated phosphorylation at Ser1177.[26,27] When HUVECs were exposed to RANKL, there was a dose-dependent increase in phosphorylation of eNOS at Ser1177 (Figure 3D). The increase was detected within 10 minutes, reached a maximum at 20 to 30 minutes, and was sustained for nearly 24 hours (Figure 3C). Consistent with this, we detected an increase in Akt phosphorylation (Figure 3C-D). However, other phosphorylation sites of eNOS were not changed by RANKL treatment (Figure S2).

We further analyzed the signaling mechanism involved in RANKL-induced eNOS phosphorylation and NO production. RANK, like other TNFR family members, lacks catalytic activity and interacts with TRAFs that act as adaptors activating downstream signaling pathways. Of the TRAFs, TRAF2 and TRAF6 appear to be important components of the RANKL signaling pathway.[28] Overexpression of DN-T6 resulted in substantial inhibition of eNOS phosphorylation, eNOS activity, and NO production, whereas DN-T2 had no effect (Figure 4A,C-D). Recruitment of TRAF6 to the cytoplasmic domains of RANK can lead to the activation of PI3K that subsequently links to Akt pathway. Indeed, the PI3K inhibitors, LY294002 and Wortmannin, markedly inhibited RANKL-induced eNOS phosphorylation, whereas PP1, a potent Src tyrosine kinase inhibitor, had no effect (Figure 4A). Consistently, overexpression of Δp85, a dominant-negative mutant of the p85 regulatory subunit of PI3K, and DN-Akt, a dominant-negative mutant of Akt, inhibited RANKL-induced eNOS activation (Figure 4B-D). Taken together, these results indicate that RANKL stimulates the production of endothelial NO via a TRAF6-dependent PI3K/Akt signaling pathway acting on eNOS.

NO is required for RANKL-induced migration and capillary-like network by ECs

RANKL induced the formation of extensive capillary-like networks of ECs cultured on 2-D Matrigel matrix, and this effect was almost completely inhibited by pretreatment with NMA (Figure 5A-B). Consistent with involvement of the eNOS activation pathway, RANKL-induced capillary-like network was blocked by Wortmannin, as well as by overexpression of DN-T6, but not of DN-T2 (Figure 5C-D). We next examined the role of NO in RANKL-induced EC migration. RANKL stimulated the chemotactic motility of HUVECs approximately 1.5-fold, and this effect was abolished by Wortmannin and NMA, as well as by DN-T6 (Figure

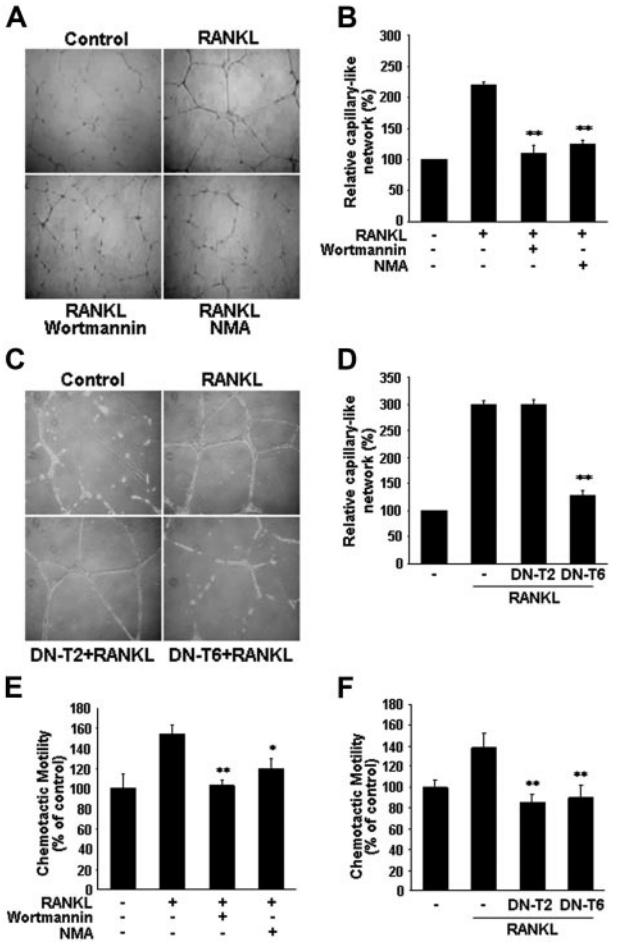

Figure 5. Involvement of PI3K/Akt-dependent NO production in RANKL-induced migration and capillary-like network by ECs. (A,E) HUVECs were preincubated for 30 minutes with or without 100 nM Wortmannin or 1 mM NMA prior to stimulation with RANKL (5 μg/mL). (C, F) HUVECs were stably transfected with DN-T2 and DN-T6 using retroviral system. (A,C) Cells were plated on Matrigel-coated plates at a density of 2×10^5 cells/well and incubated with 5 μg/mL RANKL. Microphotographs were taken after 20 hours (× 200). (B,D), Capillary-like networks were quantified with Image-Pro Plus software. (E-F) After 4 hours of incubation, chemotaxis was quantified with an optical microscopy. Three independent experiments were performed in duplicate. Data are means ± SDs; $^{*}P < .05$; $^{**}P < .01$ versus RANKL alone.

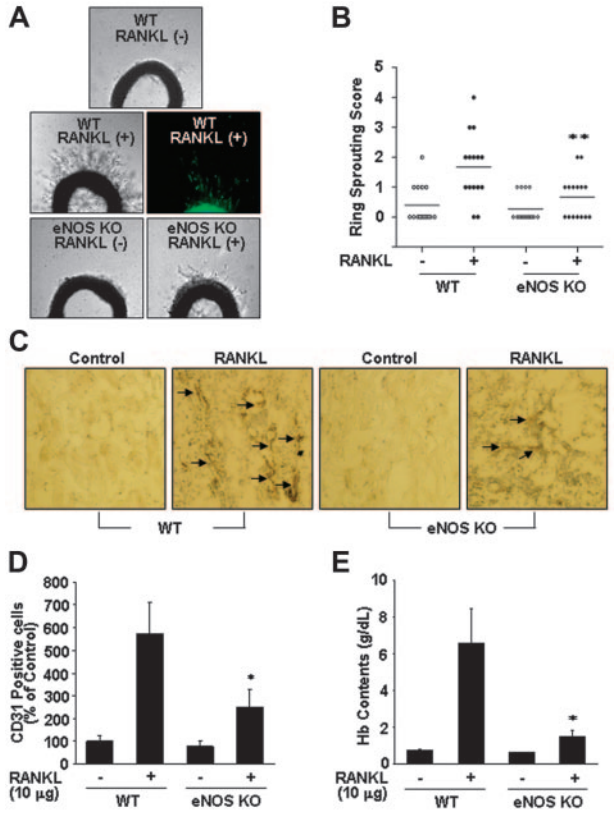

Figure 6. eNOS plays a critical role in RANKL-induced angiogenesis. (A) Aortic segments were harvested from WT and eNOS KO mice (n = 7 per group). Endothelial-cell sprouts forming branching cords from the margins of vessel segments taken from mice were photographed under a phase microscope. Staining of endothelial cells sprouted from RANKL-treated aorta with VWF (middle). (B) Sprouting scores were classified from 0 (least positive) to 5 (most positive). Data are means ± SEs. (C-E) WT and eNOS KO mice (n = 7 per group) were injected with 0.6 mL Matrigel containing RANKL (10 μg). After 7 days, the mice were killed and the Matrigel plugs were excised. (C) Plugs were stained for infiltrating endothelial cells using anti-CD31 antibody. Arrows indicate $CD31^+$ cells. (D) Quantitative assessment of $CD31^+$ endothelial cells. (E) Quantification of neovessel formation by measuring hemoglobin in the Matrigel. Data are means ± SDs; $*P < .05$; $**P < .01$ versus RANKL in WT.

5E-F). These results suggest that NO is required for the migration and differentiation of ECs in response to RANKL. In contrast to its lack of effect on EC capillary-like network, DN-T2 did inhibit the RANKL-induced increase in chemotactic motility of the HUVECs (Figure 5F), pointing to the involvement of NO-independent pathways activated by TRAF2 in RANKL-induced EC migration.

eNOS plays a critical role in RANKL-induced angiogenesis

To further assess the role of NO in RANKL-induced angiogenesis, we compared endothelial-cell sprouting in the aortic ring segments from eNOS KO and WT mice. RANKL caused a 3-fold increase in endothelial-cell sprouting in WT mice, but this effect was significantly abrogated in the aortic rings from eNOS KO mice (Figure 6A-B). Furthermore, RANKL-induced sprouting of endothelial cells in the rat aortic rings was stimulated by RANKL, and this angiogenic response was inhibited by simultaneous treatment with Wortmannin or NMA (Figure S3A-B). We further analyzed the role of endothelial cell–derived NO in RANKL-induced neovascularization in vivo. Matrigel containing RANKL was subcutaneously injected into WT and eNOS KO mice, and 7 days later the Matrigel plugs formed in the mice were excised and analyzed. There was nearly 70 g/L (7 g/dL) hemoglobin in the plugs of the WT mice, whereas those of the KO mice contained only about 18 g/L (1.8 g/dL) (Figure 6E). Plugs of the WT mice exhibited significantly higher densities of $CD31^+$ endothelial cells than those of KO mice (Figure 6C-D). Consistently, in a corneal micropocket assay, RANKL was less angiogenic in the eNOS KO mice than in the WT mice as measured by the numbers of neovessels (Figure S4A-B).

Discussion

The present results have revealed a novel action of RANKL, namely that of increasing vascular permeability in vitro and in vivo. Moreover RANKL can be added to the list of NO-dependent endothelial stimuli that promote both vascular leakage and angiogenesis. Our findings have implications for the role of RANKL in vascular physiology. Given its considerable adverse effects in adults, such as arterial calcification and inflammatory activation enhancing leukocyte adhesiveness,[5,29] our findings underline the possibility that RANKL is implicated in the development of vascular diseases.

Atherosclerosis has many characteristics in common with inflammatory disease characterized by infiltration of activated immune cells into the intima.[30] We have recently demonstrated that RANKL causes adhesion of leukocytes to ECs as a consequence of increased expression of cell adhesion molecules such as ICAM-1 and VCAM-1 in the ECs.[29] RANKL is produced by various cells, including vascular cells and activated immune cells close to blood vessels, and it exists in either a cell-bound or a secreted form.[3] Its expression, together with OPG, is also modulated by various factors such as the inflammatory cytokines, TNF-α and IL-1β.[3] Under some circumstances, the ratio of RANKL to OPG in the vascular area increases, and this change may activate endothelial cells, which are thought to be involved in promoting the early stage of atherosclerotic inflammation, which is characterized by increased endothelial permeability, up-regulation of adhesion molecules, and transendothelial migration of leukocytes.[31,32] Moreover, considering that angiogenesis and calcification are common features of advanced atherosclerotic lesions, the angiogenic and calcifying activities of RANKL may contribute to the development of atheromatous vessels.[33] Notably, this notion was supported by recent studies showing the enhanced expression of RANKL both in clinical and experimental atherosclerosis.[8] mRNA levels of RANKL were increased in T cells in patients with unstable angina accompanied by increased expression of RANK in monocytes.[8] In the $apoE^{-/-}$ mice, RANKL is significantly expressed within the atherosclerotic plaques, whereas no RANKL immunostaining was detected in the nonatherosclerotic vessel wall.[8] Furthermore, Bennett et al[9] have demonstrated that OPG inactivation results in larger and more calcified advanced lesions in the innominate arteries of older $apoE^{-/-}$ mice.

Vascular permeability is defined as the movement of fluids and molecules between blood vessels and the underlying tissues, and it is regulated by various inflammatory factors that break down intercellular endothelial junctions.[34] Although vascular leakage is not a prerequisite for blood vessel growth, increased vascular permeability often coincides with the early stage of angiogenesis and is also found in areas of diseased tissue in diabetic retinopathy, solid tumors, myocardial infarction, wounds, and chronic inflammation.[35] VEGF, originally isolated as a vascular permeability factor (VPF), is the best known angiogenic stimulus increasing the

vascular permeability of microvessels to circulating macromolecules.[16] This VPF activity is correlated with various vascular pathophysiologies.[34] In contrast, endothelial permeability is not directly affected by bFGF and PDGF, or inhibited by angiopoietin-1, despite their prominent angiogenic activities.[35,36] Our data show that the effect of RANKL on endothelial permeability is comparable to that of VEGF. Because RANKL does not increase VEGF expression in ECs,[13] RANKL-induced endothelial permeabilization and angiogenesis appear to be exerted by a direct action on ECs, independent of VEGF. Note that injection of RANKL, like VEGF, into the vitreous cavity causes breakdown of the blood-retinal barrier formed by tight junctions between the retinal vascular endothelial cells, even though the mode of action of RANKL on the retinal vasculature is unknown.

It is interesting that the effects of RANKL on ECs are so similar to those of VEGF. VEGF was originally isolated from the vasculature and was shown to play essential roles in vascular physiology during embryonic development, as well as in the evolution of various diseases of adult vasculature. It has been found that VEGF is also capable of directly enhancing osteoclastic bone resorption and promoting the survival of mature osteoclasts.[37] Conversely, although RANKL was discovered as a factor active in bone remodeling, its role in vascular disease is increasingly recognized.[38] For example, inhibition of RANKL with OPG or RANK fusion proteins or RANKL antibodies reduced chronic inflammatory disorders and malignant tumors in animal models, in addition to bone loss caused by osteoporosis.[38] Our current and previous findings that RANKL promotes vascular permeabilization, angiogenesis,[13] and proinflammatory activation provide further evidence of the adverse effects of RANKL on adult vasculature.[29]

Our data also demonstrate the prominent roles of eNOS in RANKL-induced angiogensis and vascular permeability in vitro and in vivo. Many angiogenic factors, but not all, use NO as mediator in their angiogenic effects. Treatment of ECs with RANKL increased NO production, together with increased eNOS activity (Figure 3A-B). Blockage of NO release prevented RANKL-induced EC migration and capillary-like network formation in vitro, as well as sprouting of ECs from rat aorta (Figure 5; Figure S3). Both the mouse Matrigel plug assay and the cornea micropocket assay revealed that RANKL-induced neovascularization was substantially impaired in eNOS KO animals (Figure 6; Figure S4). Thus, it is clear that NO generated from eNOS is required for angiogenic responses to RANKL. The signaling mechanism involved in vascular permeabilization is complex and involves a wide array of factors that affect cell-cell junctions, cell-matrix interaction, and cytoskeletal organization. Involvement of protein kinase C (PKC) and Rho-mediated signaling pathways has been demonstrated in the endothelial permeability induced by various stimuli.[39] NO also seems important in mediating vascular permeability, but this is context dependent. In ischemia-reperfusion injury models, NO has been shown to maintain vessel integrity.[15] However, it increased vascular permeability in tumors and in chronic inflammation.[35] Our present data indicate that NO plays an important role in RANKL-induced vascular permeability because vascular leakage in the skin of mice and in the retina induced by RANKL was significantly reduced in eNOS KO mice, and these in vivo findings were confirmed by measuring permeability and VE-cadherin junction in cultured endothelial cells. However, RANKL-induced permeability was not completely blocked by inhibiting NO production, pointing to the contribution of other signaling components such as PKC, which is activated in ECs by RANKL.[29]

RANKL causes NO production by ECs via PI3K/Akt-dependent eNOS activation (Figure 4A-D). Although eNOS is constitutively expressed in ECs, its activity can be modulated by variation in its level of expression or by reversible phosphorylation on Ser1177.[27] Treatment of ECs with RANKL did not alter the levels of eNOS mRNA and protein (Figure 3C). However, it led to phosphorylation of eNOS at Ser1177, a major phosphorylation site for Akt, and this was blocked by a dominant-negative form of Akt. Moreover, blockage of either PI3K or Akt resulted in a significant reduction in NO production in response to RANKL. Recently, we demonstrated the involvement of Src and PLC pathway in RANKL-induced angiogenesis.[13] However, the Src inhibitor PP1 had no effect on RANKL-induced eNOS activation, indicating that Src is not upstream of the Akt/eNOS pathway by RANKL. Our data also point to a predominant role of TRAF6 in the RANKL-induced NO production. Previous studies in nonendothelial cells have shown that TRAF adaptor proteins such as TRAF2, TRAF5, and TRAF6 can associate with the cytoplasmic tail of RANK and activate various intracellular signaling pathways.[28] We have recently demonstrated that TRAF2 and TRAF6 play an important role in RANKL-induced NF-κB activation in endothelial cells, which leads to increased endothelial CAM expression and EC-leukocyte interactions.[29] Surprisingly, a dominant-negative form of TRAF6 but not of TRAF2 inhibited NO production and phosphorylation of Akt and eNOS. Because PI3K mediates Akt phosphorylation, TRAF6 probably links the membrane receptor RANK to PI3K in ECs. Therefore, these results suggest a multifaceted role of TRAF6 in the RANK-mediated angiogenic and inflammatory signaling pathways in ECs.

In summary, the present study provides the first evidence that RANKL increases endothelial permeability in addition to stimulating angiogenesis as previously shown, and it reveals that these effects are dependent on endothelium-derived NO. These findings suggest that elevated RANKL levels in the vascular area may lead directly to endothelial activation and may make an important contribution to the occurrence of angiogenesis-dependent inflammatory vascular diseases such as atherosclerosis.

Acknowledgments

This work was supported by Korea Biotech R&D Group of MoST (Ministry of Science and Technology) (research grant M10416130002-04N1613-00210), the Korea Research Foundation of Korean Government (Ministry of Education and Human Resources Development [MOEHRD]) (grant KRF-2003-C00054), Molecular Cellular Biodiscovery Research Group of MoST (grant 2004-01587), and Vascular System Research Center grant from Korean Science and Engineering Foundation (KOSEF).

Authorship

Contribution: J.-K.M. and Y.-G.K. designed the research; J.-K.M., Y.-L.C., J.-H.C., Y.K., and J.H.K. performed the research; Y.-G.K. and J.R. contributed material; J.-K.M., Y.-G.K., and Y.S.Y. collected data; J.-K.M., Y.-G.K., N.M., Y.-M.K., and G.T.O. analyzed data; and J.-K.M. and Y.-G.K. wrote the paper.

Conflict-of-interest disclosure: The authors declare no competing financial interests.

Correspondence: Young-Guen Kwon, Department of Biochemistry, College of Sciences, Yonsei University, Seoul, 120-749, Republic of Korea; e-mail: ygkwon@yonsei.ac.kr.

References

1. Folkman J. Angiogenesis in cancer, vascular, rheumatoid and other disease. Nat Med. 1995;1: 27-31.
2. Moulton KS, Heller E, Konerding MA, Flynn E, Palinski W, Folkman J. Angiogenesis inhibitors endostatin or TNP-470 reduce intimal neovascularization and plaque growth in apolipoprotein E-deficient mice. Circulation. 1999;99:1726-1732.
3. Walsh MC, Choi Y. Biology of the TRANCE axis. Cytokine Growth Factor Rev. 2003;14:251-263.
4. Sattler AM, Schoppet M, Schaefer JR, Hofbauer LC. Novel aspects on RANK ligand and osteoprotegerin in osteoporosis and vascular disease. Calcif Tissue Int. 2004;74:103-106.
5. Bucay N, Sarosi I, Dunstan C, et al. Osteoprotegerin-deficient mice develop early onset osteoporosis and arterial calcification. Genes Develop. 1998;12:1260-1268.
6. Min H, Morony S, Sarosi I, et al. Osteoprotegerin reverses osteoporosis by inhibiting endosteal osteoclasts and prevents vascular calcification by blocking a process resembling osteoclastogenesis. J Exp Med. 2000;192:463-474.
7. Collin-Osdoby P. Regulation of vascular calcification by osteoclast regulatory factors RANKL and osteoprotegerin. Circ Res. 2004;95:1046-1057.
8. Sandberg WJ, Yndestad A, Oie E, et al. Enhanced T-cell expression of RANK ligand in acute coronary syndrome: possible role in plaque destabilization. Arterioscler Thromb Vasc Biol. 2006; 26:857-863.
9. Bennett BJ, Scatena M, Kirk EA, et al. Osteoprotegerin inactivation accelerates advanced atherosclerotic lesion progression and calcification in older ApoE-/- mice. Arterioscler Thromb Vasc Biol. 2006;26:2117-2124.
10. Collin-Osdoby P, Rothe L, Anderson F, Nelson M, Maloney W, Osdoby P. Receptor activator of NF-κB and osteoprotegerin expression by human microvascular endothelial cells, regulation by inflammatory cytokines, and role in human osteoclastogenesis. J Biol Chem. 2001;276:20659-20672.
11. Kartsogiannis V, Zhou H, Horwood NJ, et al. Localization of RANKL (receptor activator of NF-κB ligand) mRNA and protein in skeletal and extraskeletal tissues. Bone. 1999;25:525-534.
12. Min JK, Kim YM, Kim YM, et al. Vascular endothelial growth factor up-regulates expression of receptor activator of NF-kappaB (RANK) in endothelial cells. Concomitant increase of angiogenic responses to RANK ligand. J Biol Chem. 2003; 278:39548-39557.
13. Kim YM, Kim YM, Lee YM, et al. TNF-related activation-induced cytokine (TRANCE) induces angiogenesis through the activation of Src and phospholipase C (PLC) in human endothelial cells. J Biol Chem. 2002;277:6799-6805.
14. Rudic RD, Shesely EG, Maeda N, Smithies O, Segal SS, Sessa WC. Direct evidence for the importance of endothelium-derived nitric oxide in vascular remodeling. J Clin Invest. 1998;101:731-736.
15. Murohara T, Asahara T, Silver M, et al. Nitric oxide synthase modulates angiogenesis in response to tissue ischemia. J Clin Invest. 1998; 101:2567-2578.
16. Fukumura D, Gohongi T, Kadambi A, et al. Predominant role of endothelial nitric oxide synthase in vascular endothelial growth factor-induced angiogenesis and vascular permeability. Proc Natl Acad Sci U S A. 2001;98:2604-2609.
17. Jaffe EA, Nachman RL, Becker CG, Minick CR. Culture of human endothelial cells derived from umbilical veins. Identification by morphologic and immunologic criteria. J Clin Invest. 1973;52:2745-2756.
18. Wong BR, Rho J, Arron J, et al. TRANCE is a novel ligand of the tumor necrosis factor receptor family that activates c-Jun N-terminal kinase in T cells. J Biol Chem. 1997;272:25190-25194.
19. Lee OH, Kim YM, Lee YM, et al. Sphingosine 1-phosphate induces angiogenesis: its angiogenic action and signaling mechanism in human umbilical vein endothelial cells. Biochem Biophys Res Commun. 1999;264:743-750.
20. Oura H, Bertoncini J, Velasco P, Brown LF, Carmeliet P, Detmar M. A critical role of placental growth factor in the induction of inflammation and edema formation. Blood. 2003;101:560-567.
21. Braman RS, Hendrix SA. Nanogram nitrite and nitrate determination in environmental and biological materials by vanadium (III) reduction with chemiluminescence detection. Anal Chem. 1989; 61:2715-2718.
22. Drabkin DS, Ausin JH. Spectrophotometric constants for common hemoglobin derivatives in human, dog, and rabbit blood. J Biol Chem. 1932; 98:719-725.
23. Min JK, Lee YM, Kim JH, et al. Hepatocyte growth factor suppresses vascular endothelial growth factor-induced expression of endothelial ICAM-1 and VCAM-1 by inhibiting the nuclear factor-kappaB pathway. Circ Res. 2005;96:300-307.
24. Bazzoni G, Dejana E. Endothelial cell-to-cell junctions: molecular organization and role in vascular homeostasis. Physiol Rev. 2004;84:869-901.
25. Lee MJ, Thangada S, Claffey KP, et al. Vascular endothelial cell adherens junction assembly and morphogenesis induced by sphingosine-1-phosphate. Cell. 1999;99:301-312.
26. Shiojima I, Walsh K. Role of Akt signaling in vascular homeostasis and angiogenesis. Circ Res. 2002;90:1243-1250.
27. Dimmeler S, Fleming I, Fisslthaler B, Hermann C, Busse R, Zeiher AM. Activation of nitric oxide synthase in endothelial cells by Akt-dependent phosphorylation. Nature. 1999;399:601-605.
28. Chung JY, Park YC, Ye H, Wu H. All TRAFs are not created equal: common and distinct molecular mechanisms of TRAF-mediated signal transduction. J Cell Sci. 2002;115:679-688.
29. Min JK, Kim YM, Kim SW, et al. TNF-related activation-induced cytokine (TRANCE) enhances leukocyte adhesiveness; induction of ICAM -1 and VCAM-1 via TRAF and PKC-dependent NF-κB activation in endothelial cells. J Immunol. 2005;175:531-540.
30. Glass CK, Witztum JL. Atherosclerosis. the road ahead. Cell. 2001;104:503-516.
31. Ross R. Atherosclerosis—an inflammatory disease. N Engl J Med. 1999;340:115-126.
32. Crotti T, Smith M, Hirsch R, et al. Receptor activator NF-κB ligand (RANKL) and osteoprotegerin (OPG) protein expression in periodontitis. J Periodont Res. 2003;38:380-387.
33. Collett GD, Canfield AE. Angiogenesis and pericytes in the initiation of ectopic calcification. Circ Res. 2005;96:930-938.
34. Weis SM, Cheresh DA. Pathophysiological consequences of VEGF-induced vascular permeability. Nature. 2005;437:497-504.
35. Fukumura D, Yuan F, Endo M, Jain RK. Role of nitric oxide in tumor microcirculation. Blood flow, vascular permeability, and leukocyte-endothelial interactions. Am J Pathol. 1997;150:713-725.
36. Thurston G, Rudge JS, Ioffe E, et al. Angiopoietin-1 protects the adult vasculature against plasma leakage. Nat Med. 2000;6:460-463.
37. Nakagawa M, Kaneda T, Arakawa T, et al. Vascular endothelial growth factor (VEGF) directly enhances osteoclastic bone resorption and survival of mature osteoclasts. FEBS Lett. 2000;473:161-164.
38. Hofbauer LC, Schoppet M. Clinical implications of the osteoprotegerin/RANKL/RANK system for bone and vascular diseases. JAMA. 2004;292: 490-495.
39. Mehta D, Rahman A, Malik AB. Protein kinase C-alpha signals rho-guanine nucleotide dissociation inhibitor phosphorylation and rho activation and regulates the endothelial cell barrier function. J Biol Chem. 2001;276:22614-22620.